Amjed Abdullah[1]
Shibajyoti Ghosh Dastider[1]
Ibrahem Jasim[1]
Zhenyu Shen[2]
Nuh Yuksek[1]
Shuping Zhang[2]
Majed Dweik[3]
Mahmoud Almasri[1]

[1]Department of Electrical and Computer Engineering, University of Missouri, Columbia, MO, USA
[2]Department Veterinary Pathobiology, University of Missouri, Columbia, MO, USA
[3]Co-operative Research and Life and Physical Sciences, Lincoln University, Jefferson City, MO, USA

Received September 27, 2018
Revised November 28, 2018
Accepted November 29, 2018

Research Article

Microfluidic based impedance biosensor for pathogens detection in food products

A MEMS-based impedance biosensor was designed, fabricated, and tested to effectively detect the presence of bacterial cells including *E. coli O157:H7* and *Salmonella* typhimurium in raw chicken products using detection region made of multiple interdigitated electrode arrays. A positive dielectrophoresis based focusing electrode was used in order to focus and concentrate the bacterial cells at the centerline of the fluidic microchannel and direct them toward the detection microchannel. The biosensor was fabricated using surface micromachining technology on a glass substrate. The results demonstrate that the device can detect *Salmonella* with concentrations as low as 10 cells/mL in less than 1 h. The device sensitivity was improved by the addition of the focusing electrodes, which increased the signal response by a factor between 6 and 18 times higher than without the use of the focusing electrodes. The biosensor is selective and can detect other types of pathogen by changing the type of the antibody immobilized on the detection electrodes. The device was able to differentiate live from dead bacteria.

Keywords:
E. coli O157:H7 / Impedance biosensor / Interdigitated electrode array / Pathogen detection / *Salmonella*
DOI 10.1002/elps.201800405

1 Introduction

Foodborne diseases are a serious public health issue causing millions of acute illnesses, hundreds of thousands of hospitalizations, and thousands of deaths each year in the United States alone [1]. Many foodborne pathogens outbreaks happen every year. For example, two separate outbreaks of Shiga toxin-producing Escherichia *coli* were investigated in 2015 by FDA. These outbreaks were caused by the transmission of pathogens to humans via contaminated vegetables, fruit, meat, drinking water, and eggs. It is noted that *E. coli O157:H7* is a type of bacteria that lives in the intestines of both human and animals. It may result in bloody diarrhea and can sometimes cause kidney failure and death. There are other types of *E. coli* such as *E. coli (ETEC), E. coli (EPEC), E. coli (UPEC), and E. coli O104:H4* that can make people just as sick as E. coli *O157:H7* [2]. On the other hand, Salmonella is one of the most frequently reported cause of foodborne illness. The Salmonella family includes over 2,300 serotypes of bacteria. They are too small to be seen without a microscope. *Salmonella Enteritis* and *Salmonella Typhimurium* are the most common in the United States and account for half of all human infections. Therefore, it is of great priority and importance for the researchers to develop an advanced method for accurate and efficient detection technique of foodborne pathogenic bacteria [3].

Conventional bacterial culture testing methods are considered the gold standard for pathogens testing. They are implemented to detect and identify the pathogenic bacteria in food products and reliable for insuring food safety. These techniques have been used for many years as the food and drug administration (FDA) has established the screening procedure [4, 5]. The major disadvantage of this technique is the long duration of bacterial culture (2−5 days) to confirm diagnosis. Nucleic acid-based assays such as Polymerase Chain Reaction (PCR) have very high specificity and sensitivity and turnaround time of 24 h due to the need for enrichment step [6], Although many PCR instruments have been approved by food safety organizations such as AOAC International PCR cannot distinguish between live and dead bacteria and false positives may occur [7]. The immunological methods such as ELISA (enzyme-linked immunosorbent assay) are based on specific antibody-antigen binding and also require a long enrichment step. The failure to detect foodborne pathogens also increases the transmission risk of pathogens [8].

Some of the recent techniques that are used for biosensor detection are: (i) Electrochemical [9], potentiometric [10], impedimetric [11–13], and conductometric [14]. An electrochemical immunosensor based on screen-printed gold electrodes, for instance, was developed for the

Correspondence: Dr. Amjed Abdullah, Department of Electrical and Computer Engineering, University of Missouri, Columbia, MO, USA
E-mail: almasrim@missouri.edu

Color online: See article online to view Figs. 1–9 in color.

Table 1. Various biosensor techniques for *E. coli* and *Salmonella* detection

Technique	Food matrix	LOD [CFU/mL]	Ref.
Immunosensor/ *Salmonella* protein/ *Salmonella*	Water and Juice	1×10^1	[24]
Diazonium based/ aptasensor/ SPEs/ *Salmonella*	Apple juice	1×10^1	[19]
Impedance sensing/ IDM gold arrays/ *Salmonella*	Poultry samples	1×10^2	[20]
SPR sensor/ in-situ detection/magnetic nanoparticle/ *Salmonella*	Pure culture	1.4×10^1	[21]
Bacterial enrichment/*in-situ* /impedance detection/ *E. coli*	Chicken sample	5×10^4	[25]
Microfluidic /label free/ p-DEP focusing/ *E. coli*	Drinking water	3×10^2	[26]
Impedimetric aptasensor/ 3D-IDEA/ quantification/ *E. coli*	Water sample	1×10^2	[27]
Magnetic separation/ MNPs/ microfluidic/ *E. coli*	Pure culture	1.2×10^1	[28]
SERS/ magnetic nanoparticles/membrane filtration/ *E. coli*	Ground beef	1×10^1	[29]
Magnetic bead/sandwich complex/*in-situ* immunoassay	Spinach/chicken	1×10^1	[30]
Electrospun nanofiber/magnetic nanoparticle/ *E. coli*	Broth samples	6.7×10^1	[31]

IDM: Interdigitated microelectrode; MNPs: Magnetic nanoparticles; SERS: Surface enhanced Raman spectroscopy; SPEs: Screen printed electrodes; SPR: Surface plasmon resonance.

chronoamperometric detection of *Salmonella typhimurium* at a concentration as low as 20 cells/mL [15]. (ii) Optical, biosensors include light Surface Plasmon Resonance (SPR) [16], Surface-Enhanced Raman Spectroscopy (SERS) [17], chemiluminescence [18], and fluorescence [19]. For example, a simple and rapid SERS method was investigated for sensing *E. coli O157:H7* in ground beef at 10 CFU/mL [20]. SPR immunosensor with Fe_3O_4 MNPs separation was used for *Salmonella* enteritidis detection at a concentration as low as 14 CFU/mL [21]. (iii) Mass-based biosensors, for example, a quartz crystal microbalance nanoplatform for a label-free detection of *E. coli* was demonstrated under optimal conditions. The operation frequency was proportional to the antigen concentration with a minimum detection limit of 5 ng/mL, and a sensitivity of 0.037 Hz g/mL cm^{-1} [22]. Furthermore, Other detection techniques include magnetic nanoparticle (MNPs) which combines high surface area and high affinity, it can be implemented in biological samples labelling to provide a direct readout by naked eye in which approached the detection limit of 12 CFU/mL in broth and 30–300 CFU/mL in food matrices [23]. Electrospun detection technique combined magnetic separation technique, capillary immunoassay, and direct electrical measurement for rapid and accurate sensing of the *E. coli O157:H7* cells, the electrospun biosensor device has a linear detection for *E. coli O157:H7* concentration of 10^1 to 10^4 CFU/mL with a low concentration of 67 CFU/mL [24]. The impedimetric biosensor approach was implemented and studied (See Table 1 [19–21, 24–31]) by measuring the change in the impedance of the electrodes which indicates the presence or absence of the pathogen cells. These pathogen cells bind to the receptors such as antibodies that are immobilized on the interdigitated electrode arrays (IDEAs).

This paper presents a biosensor for rapid and accurate detection of *Salmonella* cells in raw chicken samples, and *E. coli O157:H7* cells in in pure culture. The device consists of a region for focusing and concentrating the bacterial cells, and a region for detection of bacterial cells. The detection region is coated with specific antibodies for selective detection. The *Salmonella* and *E. coli O157:H7* bacteria cells were detected with a concentration as low as 10 and 13 cells/mL, respectively.

2 Theoretical background

Dielectrophoresis (DEP) principle can be used as a competitive and alternative solution to many recent techniques of cell concentration and separation [32], such as centrifugation, filtration, fluorescence activated cell sorting, or optical tweezers. In many biomedical applications, DEP has important advantages over traditional techniques of cell separation. Using DEP principle, a wide range of cells, bacteria, viruses, DNA, protein, and particles can be isolated and analyzed without harming them. In addition, DEP can operate directly on unaltered and unlabeled cells [33]. Therefore, it reduces the expense, the labor, and the time needed for the development and validation of labeling and tagging. The cells remain viable for more analysis since DEP does not affect the properties of the cell [34]. Polarized charges will be induced on the surface of the dielectric particle when it is under an influence of an electric field (E-field). In this work, the bacteria cells were pushed to the center of the channel that is connected to the detection channel. This was achieved by adjusting the magnitude and the frequency of the applied electric field signal across the focusing electrodes using function generator while the bulk fluid kept flowing toward the outer two channels to the waste outlets. The ramp down channel generates hydrodynamic drag force on the particles/ cells that aids the focusing of cells and particles into the centerline of the channel. The DEP was discussed in details in multiple publication [35–37]. The focusing of cells is also dependent on the flow rate of the fluid inside the microchannel. DEP force in conjunction with hydrodynamic drag force creates a streamlined flow of cells, through the centerline of the microchannel towards the detection electrodes region. *E. coli* and *Salmonella* cells are captured on the detection electrode array using anti-*E. coli* and anti-*Salmonella* antibodies, respectively.

3 Materials and methods

3.1 Biosensor design

The biosensing device is shown in Fig. 1(A). It consists of (i) A focusing region, based on p-DEP, concentrate the bacterial cells in the centerline of the fabricated microchannel and push them toward the sensing region using a ramp down vertical electrode pair made of electroplated gold along with tilted thin gold finger pairs designed with 45° degree, and a ramp down channel that generates. The Implementation of this method resulted in a highly concentrated bacterial cells by adjusting the frequency and the amplitude of the signal applied on the focusing electrode. (ii) A region for bacterial cells sensing region consists of three adjacent sets of interdigitated electrode arrays (IDEAs). Each set has 10 pairs of fingers made of thin gold film. The finger width, and spacing between fingers are 10 μm, and 10 μm, respectively. Each set was measured independently using a pair of bonding pads. The focusing microchannel width begins with 300 μm and ramp down to 100 μm at the end of the focusing region. It splits into three 33 μm wide channels. The outer two channels were used as waste outlets to get rid of the bulk media that does not have bacterial cells, while the center microchannel is designed to carry the bacterial cells towards the detection region. The depth of the microchannel is 25 μm and has four inlet-outlet fluidic ports. The detection electrode was functionalized by immobilizing specific antibodies to target the pathogen cells on the electrode surface. The antibody solution was injected into the detection electrode using the antibody inlet and was immobilized on the detection electrode array. The baseline impedance of the antibody was measured. The pathogen samples were tested by flowing them through the sample inlet toward the focusing electrode and then toward the detection electrode arrays, and into the waste outlet. After the microchannel is filled with test solution, the flow stops for 30 min to achieve an efficient binding between the pathogen cells (e.g., *Salmonella* antibody) and antibodies (anti-*Salmonella* antibody). The channel was then cleaned using distilled water to remove any unbounded cells or particles. The impedance was then measured again, and the impedance change was determined by subtracting the baseline impedance values.

3.2 Biosensor microfabrication

The fabrication of the device was performed using surface micromachining process on top of a glass substrate. Fig. 1(B) shows the cross-sectional view of the fabricated layers. The glass slide (substrate) that was used in the fabrication process has a dimension of 2 inches × 1.5 inches. The substrate was cleaned using piranha solution which is composed of hydrogen peroxide (H_2O_2) and sulfuric acid (H_2SO_4) in a ratio of 1:3, respectively. The substrate was placed inside the piranha solution for 5 min to remove all the organic contamination from the substrate surface, then washed thoroughly with deionized water DI and blown dry with a nitrogen gas. After cleaning, a layer of SU-8 2005 photoresist was spin coated, followed by prebake, UV exposure without masking, post bake to achieve a thin layer with a thickness of 4 μm, and then hard baked for 30 min at 150°C to cure the SU-8 layer. This SU-8 layer improved the adhesion property between the following SU-8 layer for the microchannel, preventing the microchannel from peeling off from the substrate. Chromium (Cr) and gold (Au) layers were deposited using magnetron RF sputtering machine at 4-mTorr pressure achieving a thickness of 50 nm and 150 nm, respectively. The Au film was patterned using Shipley 1813 photoresist with a thickness of 1 μm, etched using wet etching by mixing potassium iodide (KI), iodine (I_2), and DI water to etch the exposed gold. This created the IDE array for detection region, the electrode traces, and focusing electrode, and seed layer for electroplating the side wall of the focusing region. The next step is creating a photoresist mold using AZ 4620 with a thickness of 12 μm in order to electroplate the side walls for the focusing electrode. The device was then immersed into Technic gold 25 ES gold electroplating solution to plate the gold at the focusing electrodes locations while the solution was placed on top of the hotplate and heated at 55°C, stirred at a rate of 75 rpm, and 50 μA per cm^2 current density. The deposition rate of the electroplating was controlled by the applied DC current density, and the length of the electroplating process was around 4 hh to achieve 12 μm of the electroplated gold. After electroplating, the AZ photoresist was no longer needed, and it was removed using acetone, IPA, and DI water. The Cr layer is no longer needed and was removed by placing the substrate in Cr etchant for 30 s. The following step is pattering the microchannel. SU-8 2025 photoresist was used with a thickness of 25 μm. The SU8 2025 was spin coated, soft baked, exposed to UV light, post baked, developed using SU-8 developer, and then finally hard baked to obtain the microchannel. The final step is the polydimethylsiloxane (PDMS) bonding to seal the microchannel. The microchannel was sealed using two polydimethylsiloxane (PDMS) covers cured with the fluidic connectors for the inlet and outlets. Openings were made on the first PDMS slab for the inlet and outlets, and oxygen plasma treatment was applied to make the surface hydrophilic and then SU-8 (Microchem 2005) was spin coated on the treated PDMS surface and cured at 95°C for 10 min to improve the adhesion. The device was then aligned using the inlet and the outlet markers and bonded to the first PDMS cover manually and baked on a hotplate at 95°C for 10 min while placing a weight on its top to secure the bonding. Similarly, the second PDMS cover was prepared with the fluidic connectors, treated with oxygen plasma, and aligned manually with the first PDMS layer and bonded. Fig. 1(C) shows scanning electron micrographs of the fabricated devices while Fig. 2(A) shows the completed biosensor device sealed with PDMS covers.

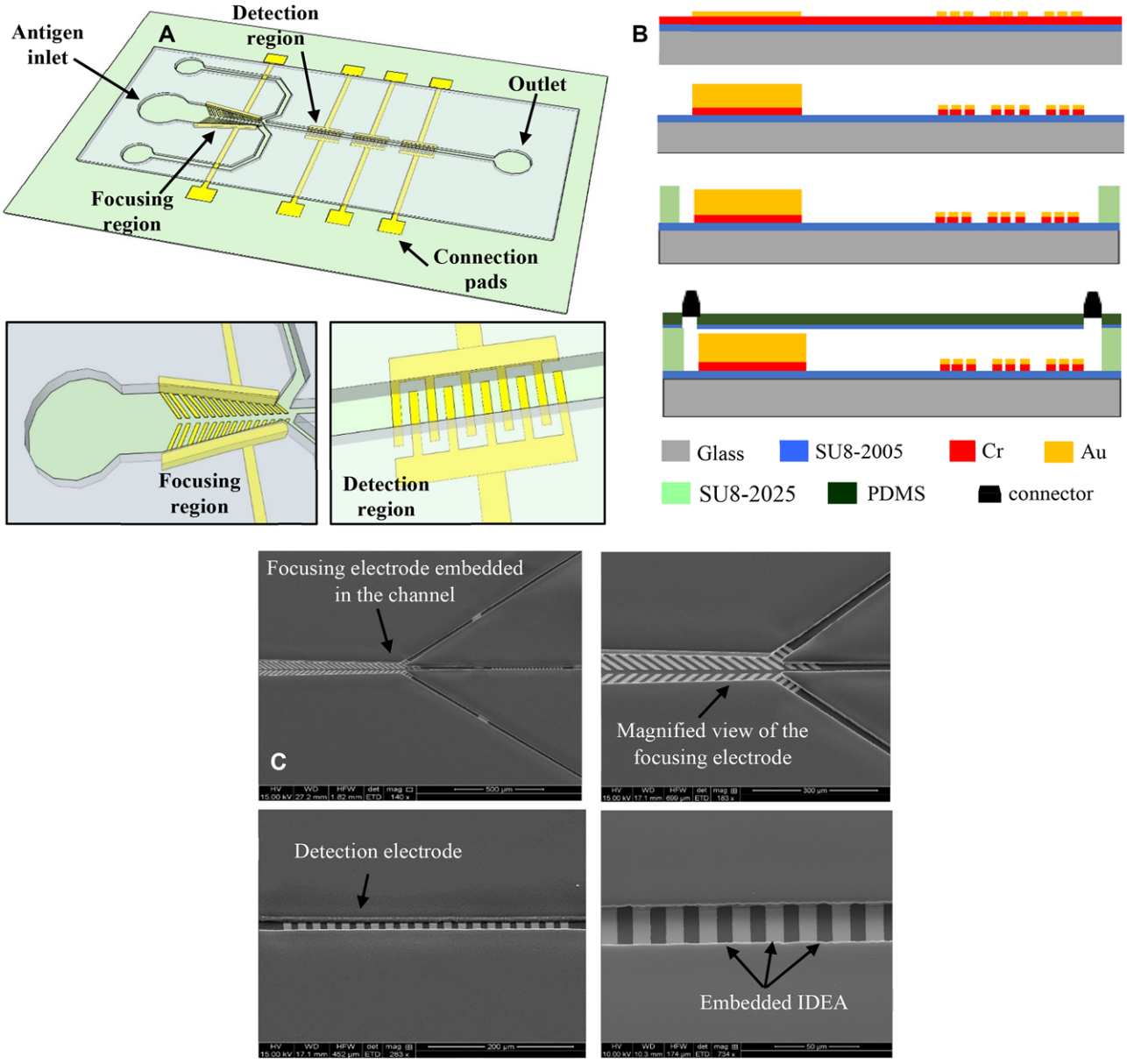

Figure 1. (A) Three dimensional schematics of the biosensor device showing the focusing and the detection regions, (B) Cross-sectional views of the biosensor fabrication processes, (C) SEM micrographs of the fabricated device showing the focusing electrodes, the detection electrodes, and the split of the microchannel.

3.3 Antibody preparation and immobilization

3.3.1 *Salmonella* antibody preparation

Rabbit *anti-Salmonella* O antiserum poly B (Becton, Dickinson and Company, Franklin Lakes, NJ) was used as capture antibody. It was mixed with the crosslinker, sulfosuccinimidyl 6-[3-(2-pyridyldithio) propionamide] hexanoate (sulfo-LC-SPDP), for antibody immobilization. The antibody was covalently bound to the biosensor gold surface through the crosslinker. Therefore, the immobilization was achieved via the crosslinker (not physical adsorption). Briefly, for each test, 8 μl of each antiserum was diluted with 292 μL filtered chicken rinse, mixed with 300 μL sulfo-SPDP (20 mM water solution), and then incubated at room temperature for 1 h. To reduce the disulfide bond of the thiolated antibody, 200 μL DTT (0.1 M sodium acetate buffer, 0.1 M NaCl, pH 4.5) was then added into the tube to react for 30 min at room temperature before the antiserum mixture was loaded into the biosensor. Therefore, antiserum was 1:100 diluted.

The thiolated antibody was immobilized on the gold surface of the three IDE arrays via the antibody inlet. Once the detection channel was filled with the antibody-crosslinker solution, the flow was stopped for 1 h, during which the

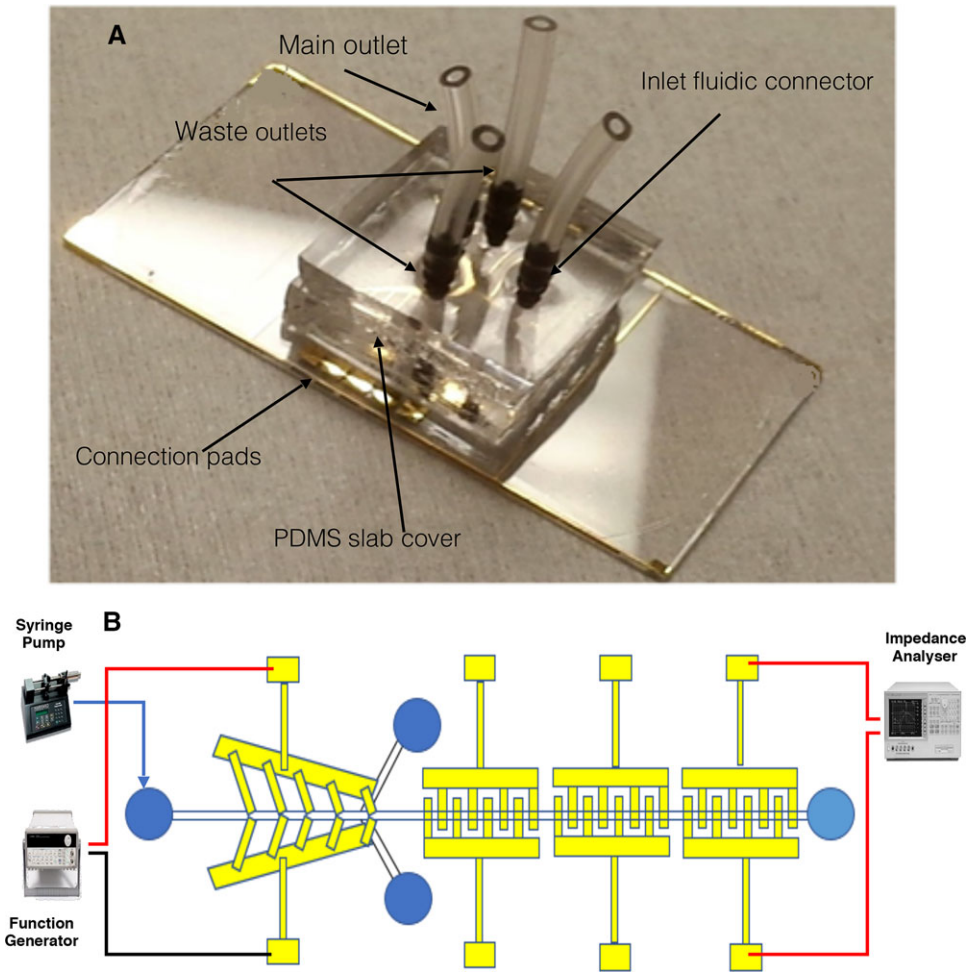

Figure 2. (A) Fabricated impedance biosensor devices sealed with PDMS slabs, (B) Schematic of the pathogen testing setup which consists of the syringe pump, the function generator, and the impedance analyzer.

antibody could be adsorbed non-specifically to the gold electrode surface. Any unbounded antibody was washed using distilled water. Next, *Salmonella* cells that corresponds to the antibody was flown over the immobilized antibody via the sample inlet. The target *Salmonella* bound to the antibody due to the specificity of the capture antibody for the *Salmonella*. Any unbound cells were washed away using distilled water, leaving the securely bonded antigen/antibody complex on the sensor array.

3.3.2 *E. coli O157:H7* antibody preparation

The *anti-E. coli O157:H7* antibody was immobilized on the detection electrodes via physisorption since the cross linker was not used. Goat anti-*E. coli O157:H7* polyclonal antibody (Ab) was purchased from Meridian life sciences, USA. The antibody was prepared at the concentration of 10 μg mL-1 using sterile DI water. 1 mL of prepared antibody was pumped into the microchannel through the inlet and the pump was stopped before the solution reached the outlet. The antibody solution was kept in the microchannel for 1 h, to achieve highest surface coverage, and minimizing any subsequent nonspecific adsorption. The anti-*E. coli* antibody was immobilized on the sensing electrode surface. After 1 h, the liquid was then pumped out, and any unbound antibodies were washed away using DI water.

3.4 Pathogen sample preparation

3.4.1 Raw chicken spiked *Salmonella* sample

The whole chicken (~5 pounds) was bought from a supermarket. Excess fluid was aseptically drained, and the carcass was transferred into a large sterile bag. A 400 mL of buffered peptone water (BPW) was poured into the cavity of the carcass. The carcass was rinsed with a rocking motion for 1 min to assure both interior and exterior surfaces were rinsed. The sample rinse was then filtered with a 100 μm and then a 20 μm cell strainer (pluriSelect Life Science, Leipzig, Germany) to remove big debris which may block the biosensor's microchannel. The filtered rinse was used freshly to dilute *Salmonella* cells or aliquoted and frozen at -20°C until used. A lab constructed avirulent *Salmonella enterica* Typhimurium strain (Δ*sipB*, Cmr) was used to spike the chicken rinse. An

overnight culture (37°C, 200 rpm, in LB broth) of *S. enterica* Typhimurium was harvested by centrifugation at 4000 rpm 10 min and washing with sterile distilled water three times and then suspended in 25% sterile glycerol. The cell suspension was aliquoted and frozen at -80°C until used. At the same time, one aliquot was serially diluted and plated on LB agar plates to determine the cell concentration. The cell concentration was determined to be 2×10^9 CFU/mL. Before the test, one aliquot *Salmonella* suspension and several aliquots of filtered chicken rinse were thawed on ice. The *Salmonella* suspension was then diluted with the filtered chicken rinse to the desired concentrations.

3.4.2 *E. coli O157:H7* Pure culture sample

The *E. coli* bacteria that is used in the study is *E. coli O157:H7* (ATCC 700728) was obtained from American Type Culture Collection (ATCC, USA). For preparing inoculum and test culture, *E. coli* (EC) broth (Fluka Analytical, USA) was used. For agar plate preparation tryptic soy agar (TSA) powder (Fluka Analytical, USA) used. Overnight broth culture of *E. coli O157:H7* measuring 1 mL was centrifuged (Horizon 642VES, Drucker Company, PA) at 3200 rpm for 10 min. After the centrifugation, the supernatant was removed, and the cells were re-dispersed in 1 mL of sterile deionized (DI) water. The re-dispersed cells were centrifuged at 3200 rpm for 10 min, and the step was repeated. After the centrifugation, the supernatant was removed, and the cells were re-dispersed in 1 mL of sterile EC broth. From the prepared inoculum, 20 μL was added to 20 mL of sterile EC broth and incubated at 37°C for 18 h (from the previous experimental analysis, it was found that 18 h incubation time is optimum). The sterile media was incubated along with the culture to be used as a "control sample". For serial dilutions, 1 mL of sample was taken and mixed well with a tube containing sterile 9 mL of sterile deionized water (per dilution). From the first dilution, 1 mL of the content was taken and mixed with 9 mL of sterile deionized water (second dilution). Subsequent dilutions were prepared similarly. Based on the bacterial concentration requirement, dilution numbers were selected for the study. For example, if the required concentration is around 10^3 Colony Forming Unit (CFU) then the sixth dilution was used, for about 10^2 CFU the seventh dilution used and for about 10–50 CFU eighth dilution was used as the test sample. These numbers derived from our routine experimentation on the bacterium. For all studies 1 mL of the sample employed in the detection process. Moreover, each sample was subjected to CFU analysis to obtain the exact bacterial concentration that was delivered to the device. A total of 1 mL of the diluted sample taken for instrumentation was subjected to spread plate inoculation on the prepared TSA plates. After inoculation, the plates were incubated at 37°C for 24 h. After incubation, the plates were observed for CFUs and the values were recorded and calculated for number of CFU present in each sample.

4 Results and discussion

4.1 Testing setup

The impedance testing setup to detect foodborne pathogens is shown in the schematic in Fig. 2(B). The following equipment are used. (i) An impedance analyzer (Agilent 4294A) with a wide frequency ranges of (100 Hz–10 MHz) were used to perform a precise measurement of the biosensor's impedance change. The device bonding pads were connected to the test leads for external connection to the impedance analyzer. (ii) A programmable infuse-withdraw syringe pump is used to infuse the test samples (antibodies and antigens) through the device inlets. The optimum flow rate to inject the test sample in the device was determined to be 1–2 μL/min. (iii) An inverted contrasting microscope was used to observe the surface of the interdigitated electrode and the microbeads as they flow through the device. A high magnification was used to study the surface of the electrodes after immobilization of the bacteria cells. (iv) A function generator was used to generate p-DEP on the focusing electrode by applying an AC voltage across the focusing electrode connection pads.

4.2 Focusing effect

The focusing region was designed to significantly improve the focusing capability of the device by getting rid of over 80% volume of the pathogens testing media. This resulted in a concentrated sample, significantly improving the pathogen detection sensitivity. It consisted of a ramp down vertical electrode pair along with tilted (with 45°) thin film finger pairs with a ramp down channel. The ramp down feature of the channel generated hydrodynamic forces that also aided the focusing process. The width of the focusing channel starts and ends at 300 and 1000 μm, respectively. This design generated p-DEP force by applying an alternating voltage of (5 V) at a specific frequency (5 MHz) that focused and concentrated the pathogenic cells or beads into the center of the microchannel and directed them toward the detection zone microchannel which has a width (30 μm) much smaller than the opening of the first focusing microchannel. The bulk fluid kept flowing toward the outer two channels into the waste outlets. The finger's width and spacing between them and spacing between the inner edges of the finger pairs were 10, 10, and 10 μm, respectively. First, the tilted thin Au finger pairs generated stronger p-DEP force. This is because the vertical Au sidewalls were far from each other and have minimum effect. Therefore, the pathogenic cells were focused in a narrow line in the center (about 10 μm wide). As the channel ramps down, the generated p-DEP force from the Au vertical sidewall pair becomes dominant especially in the z-axis and contributing more to the focusing process. Prior to injecting the pathogenic samples into the sample inlet, the three detection electrodes were functionalized with antibodies – crosslinker mixture in order to perform the selective detection of *Salmonella* and *E. coli O157: H7*. This process has increased the number

of the pathogenic cells in the detection regions because the sample media was decreased by 80% and still has the same number of pathogenic cells. When the focusing effect was not used, the number of bacterial cells that reached the detection electrode were much less. The microbeads were utilized to demonstrate the device focusing capability because their relative permittivity is 4 which is similar to that of *Salmonella* cells (4.5−6.5) [38, 39]. Optical image of the microbeads moving in the focusing region is shown in Fig. 3(A) before the p-DEP effect and in Fig. 3(B) after the p-DEP effect.

4.3 Testing results

4.3.1 Electrical equivalent circuit

To study the impedance response and the electrical properties, the equivalent circuit of the biosensor was analyzed in the presence of live and dead *Salmonella* cells separately. Fig. 3(C) represents the equivalent circuit of the impedance biosensor which consists of two double layer capacitances (C_{dl}) connected in series with the solution resistance (R_{sol}) and parallel to a dielectric capacitance (C_{de}). The electrode pair, each with an area A and spacing G were placed in parallel. An AC voltage (v) at specific frequency was applied to the electrode pair which resulted in an electrical current flow, and a solution resistance R_{Sol} given by:

$$R_{Sol} = \frac{v}{i} \rho_{Sol} \frac{G}{A} \quad (1)$$

The resistive component in the equivalent circuit is made of the test solution present between the electrodes which is represented as R_{sol}. The testing sample solution resistance R_{Sol} between the interdigitated electrode pair is proportional to the concentration of the pathogen in the tested sample. A thin layer of charged particles are formed on the surface of the electrodes due to the two separated electrodes. This thin layer of particles generates capacitance C_{dl}, while the dielectric capacitance C_{de} represents the overall capacitance of the dielectric medium. Both C_{dL} and R_{Sol} are connected in parallel with the direct capacitive coupling between the electrodes (C_{Cell}), which depends on the solution dielectric constant and the geometry of the electrodes [40, 41]. The parasitic resistors (R_{Par}) are generated from the connections and wires of the

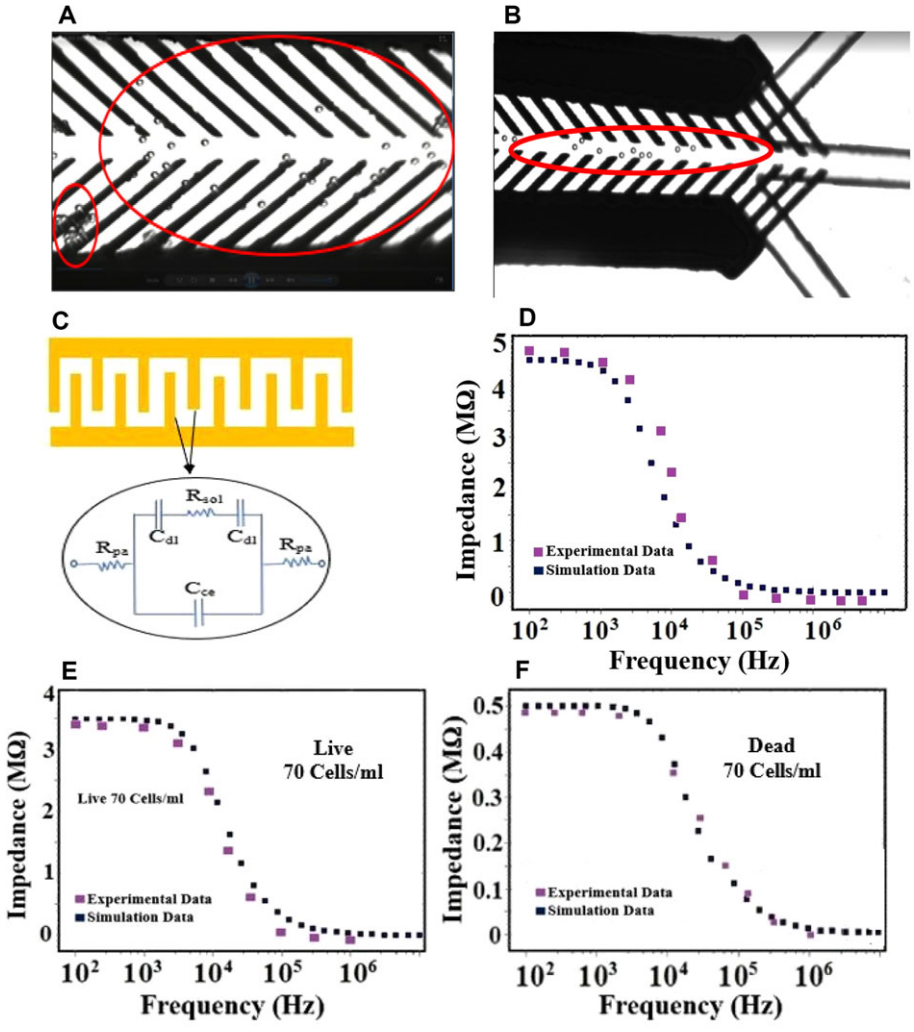

Figure 3. (A) Optical image of the microbeads moving in the focusing region before applying p-DEP forces, (B) after applying p-DEP forces, (C) Equivalent circuit of the impedance-based biosensor showing the circuit components, (D) The simulation of the equivalent circuit and the experimental results showing a good match of the experimental results with the simulated results for live *Salmonella* of 120 cells/mL, (e) live *Salmonella* of 70 cells/m and, (f) dead *Salmonella* of 70 cells/mL.

measuring circuit which is small and can be neglected. Current will flow through the R_{Sol} while another current called a displacement current flow through the capacitor C_{Cell}. The total impedance of the circuit is equal to the summation of the R_{Sol} and the two capacitors C_{dL} impedance. The total impedance is expressed by:

$$Z \approx \frac{\frac{2G}{\varepsilon_o \varepsilon_r} + J.\omega.R_{sol}}{J.\omega} \quad (2)$$

EIS spectrum analyzer software was used to simulate the response of the equivalent circuit and generate the impedance spectrum. Fig. 3(D) shows the experimental and simulated data (Bode plot) for the electrical equivalent circuit. The simulation value of C_{dl} was calculated to be around 20 nF and the value of the R_{sol} is basically the value of the tested solution resistance which is calculated to be 4.5 MΩ for the live *Salmonella* sample with the concentration of 120 cells/mL. Fig. 3(E) and (F) shows the equivalent circuit and the simulation results of the of live and dead *Salmonella* cells both with concentration of 70 cells/mL. R_{Sol} of the dead cells sample is much smaller because of the significantly low number of *Salmonella* cells bind to the electrodes. In the contrary, R_{Sol} is big in the case of live *Salmonella* cells because of the high number of cells bind to the detection electrodes. At low frequencies region (below 100 Hz) the impedance response is dominated by capacitive impedance C_{dl}. At medium frequency region (100 Hz−8 KHz) the response is due to both resistive and capacitive components and thus the R_{Sol} is dominant and the impedance is frequency independent. At high frequencies, above 8 KHz the current flow through the cell and defines the impedance value. Hence, the impedance response at high frequencies is solely due to the resistive component of the solution and the effect of bacteria cells is insignificant.

The reason that the dead cells show low impedance is that the surface of the dead cell is damaged or compromised after being exposed to the heat. The specific binding between the immobilized antibodies and the antigens cannot be formed or weakened. Unbound dead cells are then washed away during the cleaning process and the measurements were taken. Thus, there was no change or a very small change in the resistance of the solution during the dead cells testing compared with the base reading of the solution resistance of the electrodes after immobilizing the electrode with antibodies.

4.3.2 *Salmonella* spiked raw chicken testing

Different serial concentrations of *Salmonella* samples (120, 40, 15, 10) cells/mL were prepared, and the number of cells were counted based on the bacteria culturing method before injecting. The biosensor in this work is used only for detecting the presence or absence of the *E. coli O157:H7* and *Salmonella* cells. It cannot be used for cell counting. The *anti-Salmonella* antibodies with crosslinker were injected through the outlet towards the detection electrode microchannel. These antibodies were adsorbed on the detection electrode surface to ensure selective detection of *Salmonella* cells. An impedance analyzer was used to measure the impedance of the detection electrode with the antibodies injected over a frequency range of 100 Hz−10 MHz. The measured antibodies impedance was used as a baseline impedance to accurately obtain the *Salmonella* cells impedance. The biosensor device was washed with distilled (DI) water after the antibody and the bacteria injection to get rid of the unbound antibody, bacteria cells, and any unwanted material from the channel. Many experiments were performed on the *Salmonella* samples with and without applying p-DEP force. The cells were injected via the sample inlet. The flow was stopped after the channel was filled with *Salmonella* solution. The *Salmonella* was left to be immobilized on the detection electrodes for 30 mins to bind to the coated antibody recognition elements which already present on the detection electrode. An increase in the impedance values were noticed due to the antigen-antibody binding.

In addition, same experiments were repeated several times with the p-DEP focusing effect. It was used in order to push the cells toward the centerline of the microchannel and impedance measurements were recorded on the detection electrode array. Figure 4 shows the impedance spectra of the *Salmonella* samples at different concentrations with the error bars. Each error bar represents testing of 1 *Salmonella* concentration three times using three different devices. The response of the detection electrode showed that the measured impedance was directly proportional to the concentration of the *Salmonella* cells bound to the antibody on the detection electrodes. The use of the focusing electrodes has significantly improved the signal strength by a factor between 6 and 18 times than the impedance value obtained without focusing effect. It can be inferred that applying the focusing effect will increase the number of the target cells in the detection region and hence increase the chance of detecting low concentration of pathogens. Three detection electrodes were used to insure the capturing of the bacteria cells in the microchannel at a higher percentage. The impedance response as a function of frequency was calculated by subtracting the baseline impedance (antibody impedance) from the binding impedance (antigen-antibody) and the experiments were repeated 3 times to confirm the repeatability of the data. The results demonstrate that the biosensor was able to detect the *Salmonella* cells at low concentration limit of 10 cells/mL and the time required for the testing was less than 1 h excluding the antibody immobilization lifetime. In the commercial stage the fabricated device will only be used once and it is precoated with the specific antibody.

4.3.3 *E. coli O157:H7* culture testing

The device was also used to test *E. coli O157:H7* samples by using the specific *anti-E. coli* antibody without crosslinker. *E. coli O157:H7* samples were used with different concentrations (1000, 60, 25, 13) cells/mL. These samples were tested with same manner by injecting *anti- E. coli* antibody as a biorecognition element then followed by *E. coli* cells for both

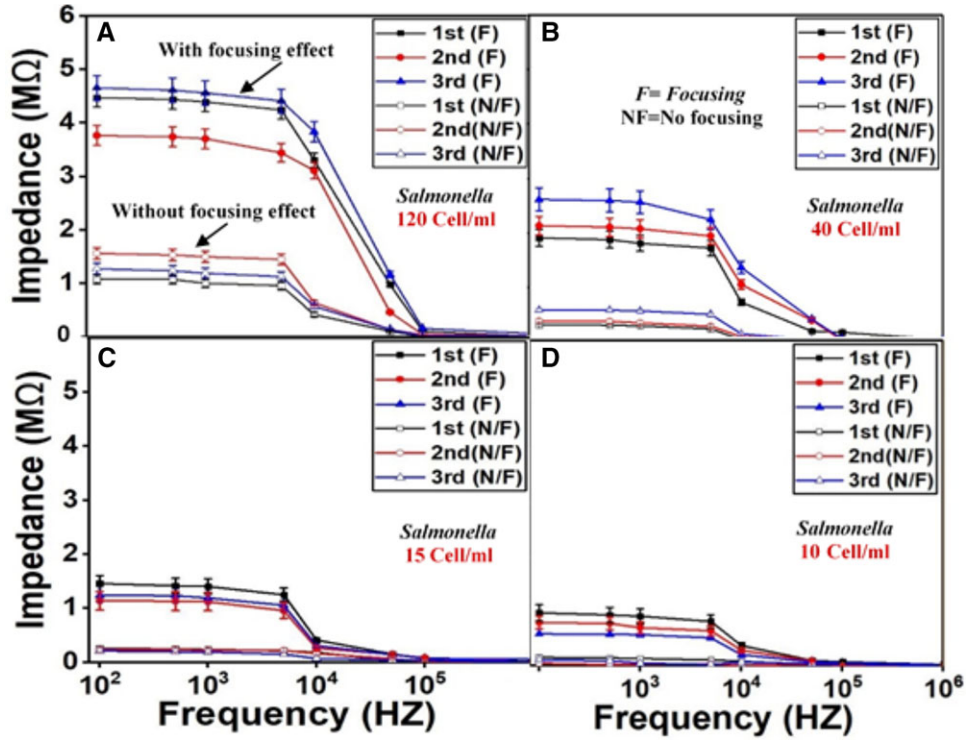

Figure 4. Testing results for *Salmonella* spiked raw chicken samples with and without focusing effect for different concentrations: (A) 120 cell/mL, (B) 40 cell/mL, (C) 15 cell/mL, (D) 10 cells/mL.

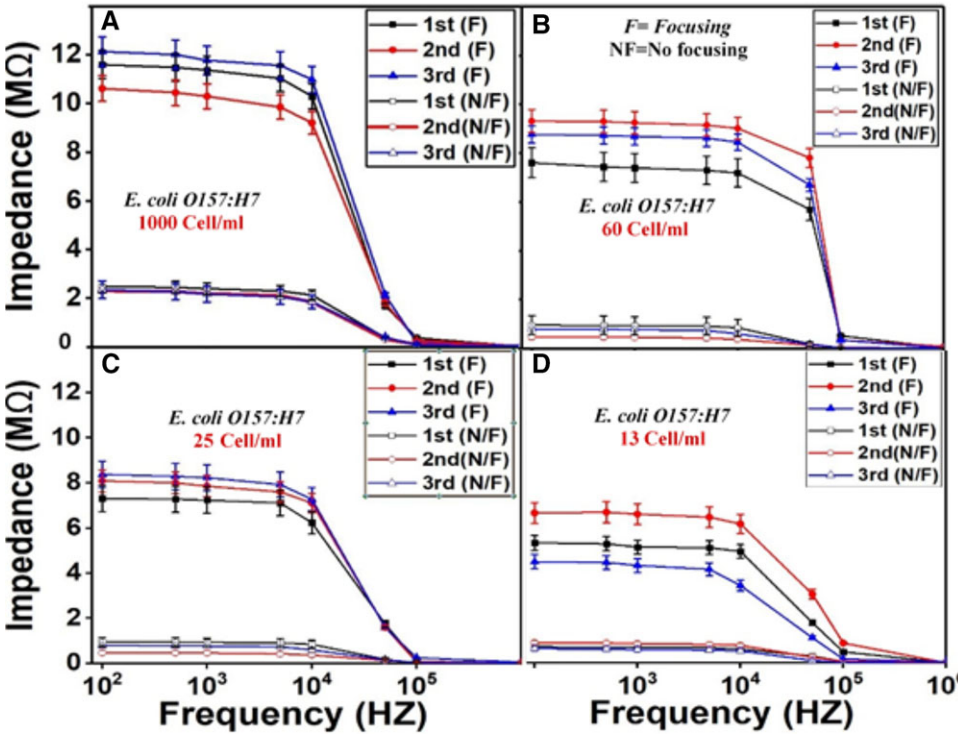

Figure 5. Testing results for *E. coli O157:H7* for different concentrations: (A) 1000 cell/mL, (B) 60 cells/mL, (C) 25 cells/mL, (D) 13 cells/mL.

with and without focusing effect. Figure 5 shows the *E. coli* testing results. The testing results of the pure culture samples demonstrate that the device was capable of detecting low concentration of *E. coli O157:H7* cells with high sensitivity and reliable results after repeating the experiments several times to confirm the repeatability of the data. Figure 6(A) and (B) shows different concentration results with and without focusing for one detection electrode for *Salmonella* cells and *E. coli O157:H7* cells respectively. The results demonstrate the significant effect of the p-DEP focusing mechanism on focus-

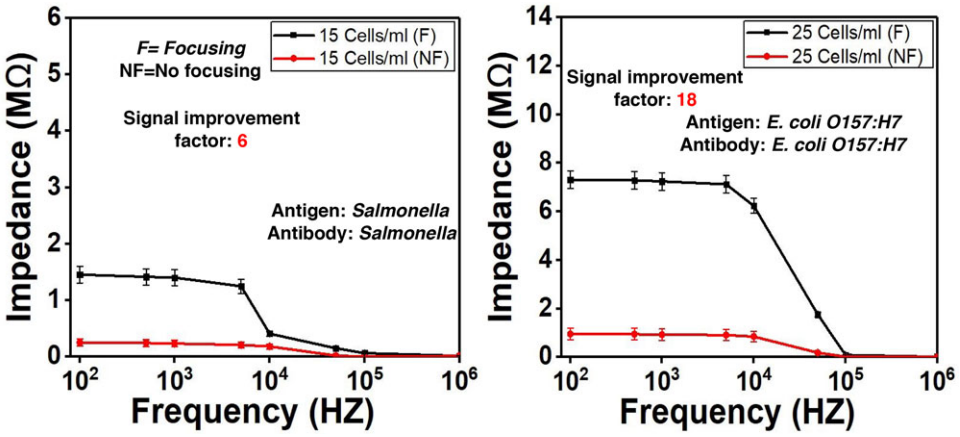

Figure 6. Comparison between focusing/ no focusing effects at various concentrations: (15 cells/mL, 25 cells/mL) for (A) *Salmonella* spiked chicken cells (B) *E. coli O157:H7* cells.

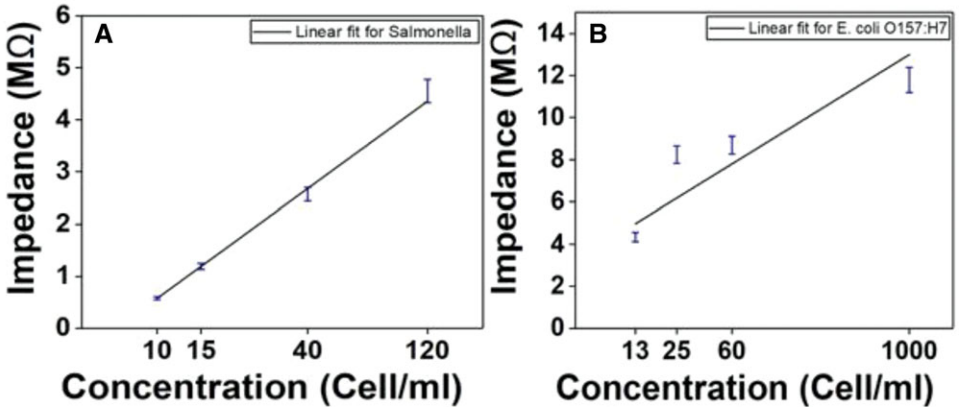

Figure 7. Comparison of impedance response of different concentrations at 1KHz for (A) *Salmonella* spiked raw chicken samples and (B) *E. coli O157:H7* samples.

ing and concentrating the *E. coli O157:H7* samples (without using crosslinker). This has enhanced the signal strength (sensitivity) as an outcome of increasing the concentration of the sample that reached the detection electrode by p-DEP. Thus, more *E. coli* cells results in more binding to antibody on the detection electrodes. The impedance response of different concentrations at 1 KHz for both *Salmonella* spiked raw chicken and *E. coli O157:H7* samples are shown in Fig. 7. The testing results shows that the impedance remains independent of frequency between 100 Hz and 8 KHz. Therefore, for the purpose of plotting the concentration as a function of impedance, a specific frequency was selected within this range. The response shows that the measured impedance is directly proportional to the concentration of the tested bacteria on the detection electrodes.

4.3.4 Specificity testing

More experiments were performed to prove the specificity of the biosensor device. This was accomplished by immobilizing *anti-E. coli O157:H7* antibody on the detection surface while the pathogenic sample was *Salmonella* cells. The impedance response showed no significant difference in the impedance values with respect to the baseline impedance of the detection electrode while the response was strong when we injected *E. coli O157:H7* cells as shown in Fig. 8(A) and (B). This was expected since the detection electrode surface was modified specifically with anti-*E. coli O157:H7* antibody, as the anti-*E. coli* antibody does not bind to non-*E. coli cells* which proves the specificity of the biosensor device. Same experiments were performed on *Salmonella* cells with concentrations of 100 cells/mL and 40 cells/mL with *Salmonella* antibody, and the impedance response showed a good signal for the *Salmonella* antigen and a weak signal response for the *E. coli O157:H7* and *O157 E. coli* (DH5 alpha) antigens of concentrations of 100 and 40 cells/mL. See Fig. 8(C) and (D).

4.3.5 Viability testing

The device ability to detect and differentiate between the live and dead cells was also investigated. The pathogen cells were killed by a brief exposure of heat at a temperature of 90°C. After that, the dead pathogen cells were injected to the device through the sample inlet toward the focusing electrode, and to the detection electrode which is coated with the antibody recognition elements. The change in impedance values was monitored for living and dead cells for different concentration of *E. coli O157:H7* and *Salmonella* cells. For the dead cells, it is clear that the change in the impedance response is very low (weak signal) compared to that of the living cells due to the

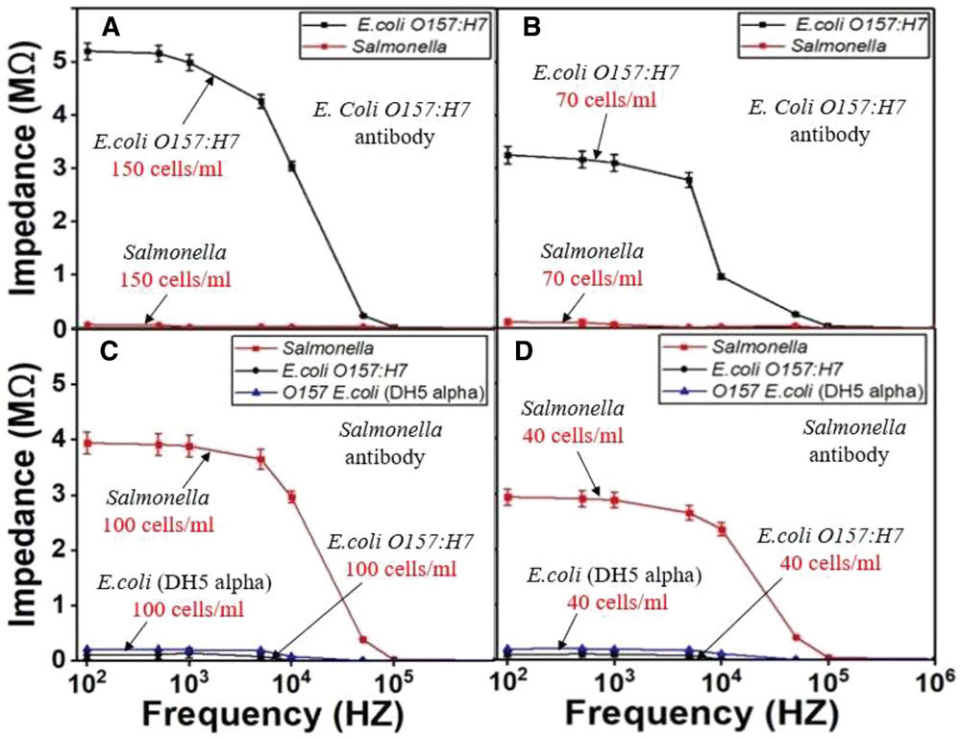

Figure 8. Specificity testing for *E. coli O157:H7* of (A) 150 cells/mL, (B) 70 cells/mL and *Salmonella* of, (C) 100 cells/mL, (D) 40 cells/mL.

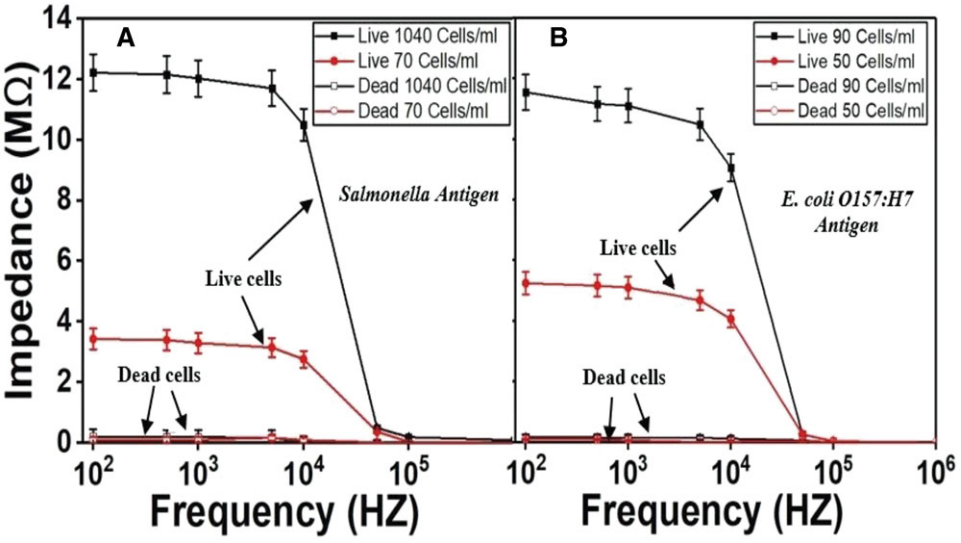

Figure 9. Differentiation capability of the device between dead and live pathogen cells testing for (1040, 90, 70, 50) cells/mL, (A) *Salmonella* cells, (B) *E. coli O157:H7* cells.

damaged cell surface after the heat exposure which diminished the chances of binding between the immobilized antibody and the dead cells. Impedance response was measured after washing the unbound dead cells through the cleaning process with DI water. Figure 9 shows the impedance response for both *E. coli O157:H7* and *Salmonella* live and dead cells. The stability of the biosensor over a long period of time and under multiple environmental conditions was not studied thoroughly. The chips are one-time use and all reagents are stored in the laboratory. However, this will be done in the future study prior to distribution of the assembled sensors to end-users.

4.3.6 Testing time duration

Prior to testing, *Salmonella* antibodies was mixed separately with the crosslinker (Sulfo-LC-SPDP) and was injected into the device via the antibody inlet for 15 min. Then, the flow was stopped and antibody−cross linker mixture was left on the detection electrodes for 1 h to achieve maximum coating. The channel was then washed for 30 min with DI water to remove the unbounded antibodies, and the impedance of each IDEA array was measured. Next, the bacterial testing sample was introduced into the biosensor via the sample inlet into the focusing region, and then toward the sensing

region. After the channel was filled, the flow was stopped for 30 min to allow the binding between the *Salmonella* antigens (type B) and *Salmonella* antibodies. After cleaning the channel with water for 30 min, the impedance was measured again, where the impedance change indicated the presence/absence of bacterial cells. Therefore, the overall testing time is 2.45 h which include the antibody coating time, antigens binding time and the multiple washing step time. It is noted that the biosensor will be used as a disposable device to eliminate the possibility of contamination, per the recommendation of food processing companies including major poultry industry such as Tyson, Cargill, and Pilgrim's. The device must be pre-coated with antibody cross linker mixture prior to sale. Therefore, the testing time that will be counted is the testing and washing step time, which is 1 h.

5 Concluding remarks

The work presented in this paper involves a MEMS biosensor based on impedance spectroscopy for the detection of *E. coli O157:H7* and *Salmonella* cells in raw chicken samples. The device design consists of focusing electrode pair with a ramp down channel, and detection electrode arrays coated with specific antibody with and without a crosslinker. The p-DEP force was applied in order to focus and concentrate the bacterial cell to a detectable level. The results demonstrate that the device has a limit of detection of 10 cells/mL, and 13 cells/mL for *Salmonella*, and *E. coli*, respectively. The inclusion of the focusing region has improved the signal sensitivity by a factor between 6 and 18 times. In addition, the selectivity measurement demonstrates the device ability to distinguish between pathogens based on the antibody. The viability measurement also demonstrated that the device can distinguish between live and dead bacterial cells. Finally, the detection time was less than 1 h.

This project is supported in part by National Science Foundation Grant No. ECCS-0925612, and USDA-Capacity Building Grant.

The authors have declared no conflict of interest.

6 References

[1] Centers for Disease Control and Prevention, *Escherichia coli* O26 infections linked to Chipotle Mexican grill restaurants (Final Update), November 2015; https://www.cdc.gov/ecoli/2015/o26-11-15/index.html.

[2] Canizalez-Roman, A., Flores-Villaseñor, H. M., Gonzalez-Nuñez, E., Velazquez- Roman, J., Vidal, J. E., Muro-Amador, S., León-Sicairos, N., *Front. Microbiol.* 2016, *7*, 1924.

[3] Law, J. W. F., Ab Mutalib, N. S., Chan, K. G., Lee, L. H., *Front. Microbiol.* 2015, *5*, 770.

[4] Lee, K. M., Runyon, M., Herrman, T. J., Phillips, R., Hsieh, J., *J. Food Control* 2015, *47*, 264–276.

[5] Wu, W., Zhao, S., Mao, Y., Fang, Z., Lu, X., Zeng, L., *Anal. Chim. Acta* 2015, *861*, 62–68.

[6] Salihah, N. T., Hossain, M. M., Lubis, H., Ahmed, M. U., *J. Food Sci. Technol.* 2016, *53*, 2196–2209.

[7] Barbau-Piednoir, E., Mahillon, J., Pillyser, J., Coucke, W., Roosens, N. H., Botteldoorn, N., *J. Microbiol. Methods* 2014, *103*, 131–137.

[8] Crim, S. M., Iwamoto, M., Huang, J. Y., Griffin, P. M., Gilliss, D., Cronquist, A. B., Lathrop, S., *Morbidity Mortality Weekly Rep.* 2014, *63*, 328–332.

[9] Vásquez, G., Rey, A., Rivera, C., Iregui, C., Orozco, J., *Biosens. Bioelectron.* 2017, *87*, 453–458.

[10] Gehring, A. G., in *High Throughput Screening for Food Safety Assessment* (Eds.: Bhunia, A. K., Kim, M. S., Tait, C. R.), Elsevier, Cambridge UK, 2015, pp. 301–314.

[11] Kim, G., Moon, J. H., Moh, C. Y., Lim, J. G., *Biosens. Bioelectron.* 2015, *67*, 243–247.

[12] Dastider, S. G., Barizuddin, S., Dweik, M., Almasri, M., *RSC Adv.* 2013, *3*, 26297–26306.

[13] Abdullah, A., Jasim, I., Alalem, M., Dweik, M., Almasri, M., *Proc. IEEE Int. Conf. Micro Electro Mech. Syst.* 2017, 381–385.

[14] Adley, C. C., Ryan, M. P., in *High Throughput Screening for Food Safety Assessment* (Eds.: Bhunia, A. K., Kim, M. S., Tait, C. R.), Elsevier, Cambridge UK, 2015, 315–326.

[15] Sheikhzadeh, E., CHamsaz, M., Turner, A. P. F., Jager, E. W. H., Beni, V., *Biosens. Bioelectron.* 2016, *80*, 194–200.

[16] Nguyen, H., Park, J., Kang, S., Kim, M., *Sensors* 2015, *15*, 10481–10510.

[17] Dina, N. E., Zhou, H., Colniţă, A., Leopold, N., Szoke-Nagy, T., Coman, C., Haisch, C., *Analyst* 2017, *142*, 1782–1789.

[18] Ali, Z., Wang, J., Tang, Y., Liu, B., He, N., Li, Z., *Biomater. Sci.* 2017, *5*, 57–66.

[19] Cho, I. H., Mauer, L., Irudayaraj, J., *Biosens. Bioelectron.* 2014, *57*, 143–148.

[20] Cho, I. H., Bhandari, P., Patel, P., Irudayaraj, J., *Biosens. Bioelectron.* 2015, *64*, 171–176.

[21] Liu, X., Hu, Y., Zheng, S., Liu, Y., He, Z., Luo, F., *Sens. Actuators B* 2016, *230*, 191–198.

[22] Nehra, A., Pandey, K., Singh, K. P., Ahalawat, S., Joshi, R. P., *Anal. Lett.* 2017, *50*, 1897–1911.

[23] Suaifan, G. A., Alhogail, S., Zourob, M., *Biosens. Bioelectron.* 2017, *92*, 702–708.

[24] Luo, Y., Nartker, S., Wiederoder, M., Miller, H., Hochhalter, D., Drzal, L. T., Alocilja, E. C., *IEEE Trans. Nanotechnol.* 2012, *11*, 676–681.

[25] Yao, L., Wang, L., Huang, F., Cai, G., Xi, X., Lin, J., *Sens. Actuators B* 2018, *259*, 1013–1021.

[26] Kim, M., Jung, T., Kim, Y., Lee, C., Woo, K., Seol, J. H., Yang, S., *Biosens. Bioelectron.* 2015, *74*, 1011–1015.

[27] Liu, H. T., Wen, Z. Y., Xu, Y., Shang, Z. G., Peng, J. L., Tian, P., *Mod. Phys. Lett. B* 2017, *31*, 1750233.

[28] Wen, T., Wang, R., Sotero, A. F., Li, Y., *2017 ASABE Annual International Meeting of the American Society of Agricultural and Biological Engineers*, Spokane, Washington July 16–19, 2017, American Society of Agricultural and Biological Engineers, St. Joseph, MI; p. 1. https://doi.org/10.13031/aim.201700368. 2017.

[29] Bagheryan, Z., Raoof, J. B., Golabi, M., Turner, A. P., Beni, V., *Biosens. Bioelectron.* 2016, *80*, 566–573.

[30] Mutreja, R., Jariyal, M., Pathania, P., Sharma, A., Sahoo, D. K., Suri, C. R., *Biosens. Bioelectron.* 2016, *85*, 707–713.

[31] Brosel-Oliu, S., Ferreira, R., Uria, N., Abramova, N., Gargallo, R., Muñoz-Pascual, F. X., Bratov, A., *Sens. Actuators B* 2018, *255*, 2988–2995.

[32] Gagnon, Z. R., *Electrophoresis* 2011, *32*, 2466–2487.

[33] Bai, G., Li, Y., Chu, H. K., Wang, K., Tan, Q., Xiong, J., Sun, D., *Biomed. Eng. Online* 2017, *16*, 41.

[34] LaLonde, A., Romero-Creel, M. F., Lapizco-Encinas, B. H., *Electrophoresis 20*15, *36*, 1479–1484.

[35] Song, H., Rosano, J. M., Wang, Y., Garson, C. J., Prabhakarpandian, B., Pant, K., Lai, E., *Lab Chip* 2015, *15*, 1320–1328.

[36] Moon, H. S., Kwon, K., Kim, S. I., Han, H., Sohn, J., Lee, S., Jung, H. I., *Lab Chip* 2011, *11*, 1118–1125.

[37] Qian, C., Huang, H., Chen, L., Li, X., Ge, Z., Chen, T., Sun, L., *Int. J. Mol. Sci.* 2015, *15*, 18281–18309.

[38] Esteban-Ferrer, D., Edwards, M. A., Fumagalli, L., Juárez, A., Gomila, G., *ACS Nano* 2014, *8*, 9843–9849.

[39] Liu, J., Jasim, I., Abdullah, A., Shen, Z., Zhao, L., El-Dweik, M., Almasri, M., *Sci. Rep.* 2018, *8*, 16109.

[40] Zang, F., Gerasopoulos, K., Fan, X. Z., Brown, A. D., Culver, J. N., Ghodssi, R., *Biosens. Bioelectron.* 2016, *81*, 401–407.

[41] Ibrahim, M., Claudel, J., Kourtiche, D., Nadi, M., *J. Electr. Bioimped.* 2013, *4*, 13–22.